

Non-exponential photocurrent growth and decay in Safranine-T dye doped solid state polymer photoelectrochemical cell

S. K. DEY, MD. R. ISLAM, N. B. MANIK*, A. N. BASU
 Condensed Matter Physics Research Centre, Department of Physics,
 Jadavpur University, Calcutta 700 032, India
 E-mail: nb_manik@yahoo.com
 E-mail: nabin@juphys.ernet.in

In the present communication photoconductivity has been studied in Safranine-T dye doped solid state polymer photoelectrochemical cell (PEC). The cell contains a blend made of Safranine-T dispersed in polyvinyl alcohol (PVA), polyethylene oxide (PEO) complexed with ammonium perchlorate (NH_4ClO_4), ethylene carbonate (EC) and propylene carbonate (PC). A thin layer of this blend is sandwiched between two ITO coated glass plate electrodes. The photoresponse is observed in our system illuminated by a tungsten lamp in presence of an external bias voltage. Photocurrent changes with the applied bias voltage and the typical change is about $1.68 \mu\text{A}$ for a device area of 0.64 cm^2 at a bias voltage of 1.5 V and at an incident intensity of about 40 mW/cm^2 which indicates a sensitivity of $0.66 \times 10^{-4} \text{ A/W}$. In the present work the dark current–voltage (I - V) characteristic and the variation of the photocurrent with time have been investigated. At low operating voltage the I - V characteristic is ohmic while at high bias voltage an exponential distribution of trap centers gives a good fit to the dark I - V characteristic. The experimental results show a non-exponential growth and decay of photocurrent with rich structure which may indicate a dispersive transport in such disordered amorphous systems. The dispersive transport model has been applied to explain qualitatively the experimental findings of this non-exponential photocurrent behaviour. The experimental data are fitted with a power law function as $I_{\text{ph}}(t) \propto t^\alpha$ for photocurrent growth and $I_{\text{ph}}(t) \propto t^{-\beta}$ for decay where $I_{\text{ph}}(t)$ is photocurrent and α and β are some constants at a particular bias voltage. The observed slow response speed of the device may be due to slow diffusion of ions as well as the immobilization of charge carriers at deep traps. The present investigation will be helpful to understand the performance of the device and the charge transport mechanism in dye doped solid state polymer electrolyte cell. © 2003 Kluwer Academic Publishers

1. Introduction

Recently organic and polymer photoconductors have been widely used for large area optoelectronic devices such as xerographic photoreceptors and photodetectors [1–14], solar cells [15–18] etc. In these applications generally photoconductive amorphous thin films including molecularly doped polymers dispersed in a polymer matrix are sandwiched between two metallic electrodes at least one of which is a transparent conductor. Upon application of incident radiation of suitable wavelength photocarriers are generated and these carriers are separated under applied electric field. The photoconductivity study of organic/polymer materials and the uses of them as organic photoreceptors have been reviewed recently [1, 8]. Transient photoconductivity has also been investigated by different workers [9, 10] in

single and multi layer sandwiched structure in different organic materials. Steady state growth and decay of current for X-ray radiation in different organic films are also available in literature [18–20]. Some theoretical models have also been developed by different workers to describe the photocurrent behaviours in organic/polymer based materials [21–23]. It is found that most of these works have been done mainly in layered structures in which a single or multilayer films of organic/polymer material are sandwiched between the two electrodes. However, the study of steady state photoconductivity measurement in solid state photoelectrochemical cell (PEC) in visible range is rather scarce.

In our earlier works [24, 25] we have reported that the solid state dye doped conducting polymer PEC can

* Author to whom all correspondence should be addressed.

be used for light detection. The PEC under study contains a blend made of Safranin-T dispersed in transparent polyvinyl alcohol (PVA), polyethylene oxide (PEO) complexed with ammonium perchlorate (NH_4ClO_4), ethylene carbonate (EC) and propylene carbonate (PC). Safranin-T dye is used as an optical active material and is dispersed in PVA which acts as an inert binder. NH_4ClO_4 is mixed with a solid polymer matrix PEO to form the solid state ionic conductor. The ionic conductivity of PEO: NH_4ClO_4 complexes is very low [16, 26] for ambient temperature application. The use of a plasticizer is a common technique to enhance the ionic conductivity [16]. In this system we have used EC dissolved in PC as plasticizers to enhance the mobility of the charge carriers. A solid film of the blend is sandwiched between two transparent Indium Tin Oxide (ITO) coated glass plates as the contact electrodes. Incorporation of mobile ions in this blend changes the operational characteristics of the device drastically with respect to conventional single or multi-layered structure. It is expected that the positive ions from NH_4ClO_4 salt are accumulated near the cathode and the negative ions near the anode upon application of external bias on the device. A depletion layer is formed inside the active layer due to the redistribution of ionic charges in a similar manner as found in recent work on light emitting electrochemical cell [27–35] used to develop organic light emitting diodes. Upon illumination from a light source dye molecules absorb light and photocarriers are generated. These photocarriers are then separated by the external field applied on the device. It is expected that the internal field produced by the redistribution of the ion species within the PEC enhances the migration process of these photocarriers. The barrier potential in contacts of ITO and polymer materials is lowered [33, 35] due to the accumulation of these ion species near the respective electrodes leading to enhancement of charge injection through the metal polymer interface layer.

In this work, we have studied the dark current–voltage (I - V) characteristic and the photocurrent growth, saturation and decay behaviour to understand the charge transport mechanism of the device. Once the photocarriers are generated different processes like charge trapping, recombination etc. determine the observed photoconductivity. The photoconductivity study is important to understand the complex charge transport processes occurring in these disordered materials. The nature of the distribution of traps is determined from the dark I - V characteristic and is found to be exponential in nature. Our experimental results show a non-exponential growth and decay of the photocurrent. The experimental data are fitted with a power law function of the form $I_{\text{ph}}(t) \propto t^\alpha$ for photocurrent growth and $I_{\text{ph}}(t) \propto t^{-\beta}$ for decay where $I_{\text{ph}}(t)$ is the photocurrent and α and β are constants which depend on bias voltage. Here, attempt has been made to explain this non-exponential behavior of photocurrent by using a dispersive transport model for a disordered system originally developed by Scher and Montrol [23] and further extended by other workers [19–20]. The non-exponential type of growth and decay of photocurrent indicates a complex transport mechanism of charge carriers.

2. Experiment

The structure of the dye, Safranin-T (E. Merck, Germany) having absorption peak at 520 nm which corresponds to an optical band gap of the order of 2.39 eV is shown in Fig. 1a. The dye was recrystallised twice from ethanol–water mixture and mixed with PVA (S. D. Fine Chem. Ltd., Boisar; M. W. 125000). 5 gm of PVA was mixed with 10 cc of double distilled water, warmed gently and stirred to make a transparent viscous solution of PVA. 1 mg of Safranin-T was mixed with this solution. A solid electrolyte was prepared by mixing PEO (BDH, England; M. W. 600000)– NH_4ClO_4 (Fluka, 99.5% pure)–EC (Fluka, 99.5% pure) and PC (Fluka, 99.5% pure). The complex of PEO (NH_4ClO_4)–EC–PC (30.60%–3.60%–19.60%–46.20% by weight) were mixed, stirred and heated around 80°C for 5 hrs. This gel like solid electrolyte was mixed with the previously prepared dye-PVA solution to form the blend. This blend was heated about 80°C and stirred properly to mix well for about 2 hrs. This blend is sandwiched between two transparent ITO coated glasses which were previously cleaned in chloroform solution and dried under vacuum for about 5 hrs. The uniform film thickness was controlled by placing two teflon spacers of thickness about 2 μm near the edges of the electrodes and two spring clips were fixed at a moderate pressure at the ends of the electrodes. The active device area was measured to be of the order of 0.64 cm^2 . The two electrical leads were taken out from the two ends of the ITO coated glass. The structure of the PEC is shown in Fig. 1b. A schematic diagram of the experimental set up is indicated in this figure.

The cell is biased with a dc source with a series resistance of 47 $\text{K}\Omega$. The current flowing through the device was estimated by measuring the voltage drop (measured by a Philips 4 1/2 digit Multimeter) across this sensing resistance. Dividing the measured voltage by the value of this sensing resistance, the current flowing through

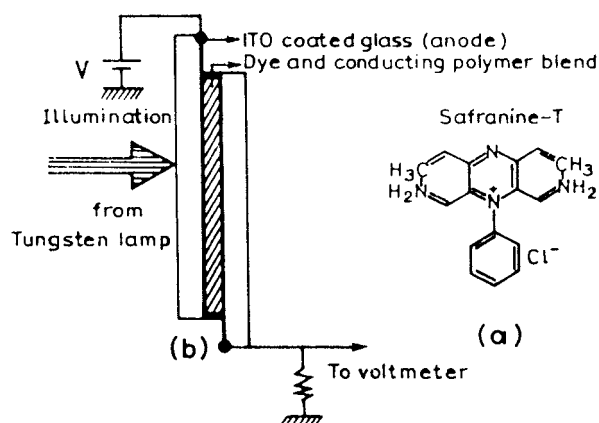


Figure 1 (a) Structure of Safranin-T which is a fluorescence cationic dye soluble in water with a peak absorption at a wavelength 550 nm. (b) Structure of the photoelectrochemical cell. A 2 μm thin film blend made of organic dye Safranin-T, polyethylene oxide (PEO) complexed with ammonium perchlorate (NH_4ClO_4), ethylene carbonate (EC) and propylene carbonate (PC) is sandwiched between two ITO coated glass plate electrodes. The ITO coated glass plates are connected to the external voltage source. Polychromatic light from a tungsten lamp is allowed to incident on the device for optical measurement. The effective device area is 0.64 cm^2 .

the device is calculated. It is observed that after application of each bias voltage a sufficient time (about 20 minutes) is required to attain the steady value of the current. The reading has been taken after attaining the steady value.

For optical measurement light from a tungsten lamp of 200 W is allowed to incident on the biased cell. Light is allowed to pass through a water filter to avoid the excess heating of the device. The distance of the lamp from the sample is so adjusted that an intensity of about 40 mW/cm² is incident on the device. The intensity is measured by a calibrated lux meter (Kyoritsu Electrical Instruments Works Ltd. Tokyo, model 5200). It is observed that due to incident radiation voltage drop across the sensing resistance is increased and attains a saturation value which is recorded with time. After attaining the saturation value the light is switched off. As soon as the light is switched off the reading of the multimeter begins to fall and reaches almost the initial dark value. The measurement is repeated and the reproducibility of the measurement has been checked for number of times for different bias voltages.

3. Results and discussion

3.1. Steady state dark I - V characteristic

A logarithmic plot of the bias current vs. voltage is shown in Fig. 2. The $\ln I$ - $\ln V$ plot shows a transition point at a bias voltage of 1.1 V which seems to indicate a change in charge conduction mechanism. Inset of Fig. 2 shows the linear plot of current vs. bias voltage. The I - V characteristic is symmetric about the origin for both forward and reverse biases. The I - V characteristic by changing the polarity of the dc bias is not shown in this figure.

Due to their weak molecular bonds and structural disorder organic materials are prone to have electronic traps. These traps introduce additional energy levels inside the energy gap between the lowest unoccupied

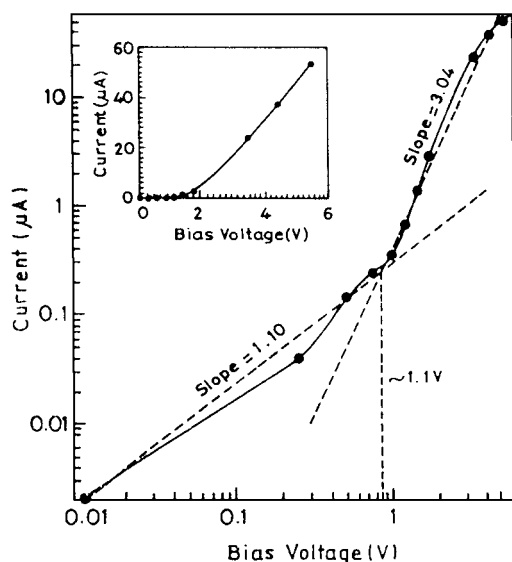


Figure 2 Logarithmic plot of current vs. bias voltage in the dark. The I - V characteristics can be found to have the form $I \sim V^{(m+1)}$ where $m = T_t/T$, T_t is the characteristics temperature of the traps and T is the room temperature. With a best fit to our experimental data the values of m are found to be 0.11 and 2.04 below and above bias voltage 1.1 V.

molecular orbital (LUMO) states and highest occupied molecular orbital (HOMO) states. Charging and discharging of these trap levels can play a key role in operation and performance of the device made of organic and polymer materials. These trap levels have a major role to determine the I - V characteristics [36–39]. In fact the distribution of the trap levels may be estimated from the I - V characteristic. To deduce I - V relation the starting equations i.e., one-dimensional drift current and Poisson equations can be written as [36],

$$J = nq\mu E \quad (1)$$

and

$$\partial n / \partial x = -q / \varepsilon (n + n_t) \quad (2)$$

where J is the current density, μ is the carrier mobility, E is the electric field strength, n and n_t are the free and trapped charge concentrations respectively, q is the electronic charge, and ε is equal to $\varepsilon_0 \varepsilon_r$ with ε_0 being the permittivity of vacuum and ε_r the relative dielectric constant of the material. Depending on the trap energy distribution it is found that I - V relation may appear in the following forms [36]: (i) $I \sim V$ for low operating voltage region which indicates ohmic conduction process, (ii) $I \sim V^2$ which indicates the space charge or discrete trap charges limited conduction and (iii) $I \sim V^{m+1}$ for exponential distribution of trap charges, where m is a constant and is given by $m = T_t/T$, T_t and T are the characteristic temperature of the trap distribution and room temperature respectively. In regime (iii) the trap charge concentration (n_t) is expressed in the following form,

$$n_t = H_n \exp(F_n / K T_t) \quad (3)$$

where H_n is the trap density, F_n is the electron Fermi energy, K is the Boltzmann's constant and T_t is the characteristic temperature of the trap distribution given by $T_t = E_t / K$, where E_t is the characteristic trap energy.

Our experimental data can be fitted as $I \sim V^{1.10}$ and $I \sim V^{3.04}$ below and above the bias voltage 1.1 V respectively. So, from the observation it may be concluded that current conduction process is ohmic below 1.1 V and above it the conduction process is governed by trap charges with an exponential energy distribution. Further details of the trap levels are under study.

3.2. Photocurrent behaviour

The variation of photocurrent (I_{ph}) with time (t) for different bias voltages is shown in Fig. 3 Photocurrent changes with the bias voltage and the typical change (i.e., saturation photocurrent minus the initial dark value) is about 1.68 μ A for the device area of 0.64 cm² at a bias voltage of 1.5 V and at an incident intensity of about 40 mW/cm². The sensitivity as calculated from these data is 0.66×10^{-4} A/W. The photocurrent-time (I_{ph} - t) curve has three distinct regions: growth (from M to N), saturation (from N to O), and decay (from O to P) as shown in this figure. It is interesting to note that the response speed of the device is very slow. The growth time (to reach from M to N) and decay time (to reach from O to P) are 600 sec and 800 sec respectively. The variation of this photocurrent in different regions

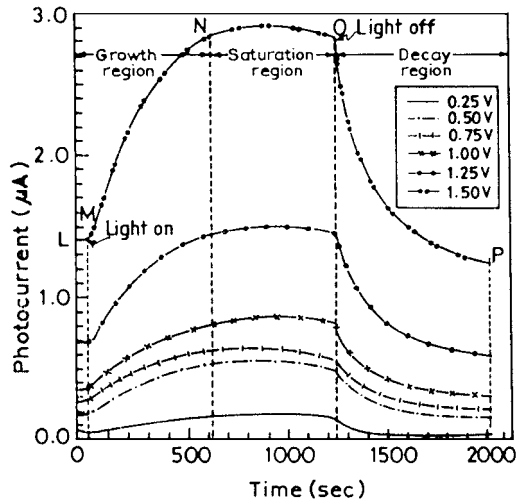


Figure 3 Photocurrent variation with time for different bias voltage. The growth and decay of photocurrent is measured as follows. The cell is biased with a voltage source making any one ITO electrode as anode. After attaining a steady dark current (portion L to M) the cell is illuminated from a polychromatic tungsten light source of radiation intensity 40 mW/cm^2 . As soon as the light is switched on the photocurrent begins to rise (portion M to N) and attains a saturation value (portion N to O). After the saturation the light is switched off and the photocurrent decays almost to its initial value (portion O to P). Time taken to reach from M to N and O to P is about 600 and 800 sec respectively.

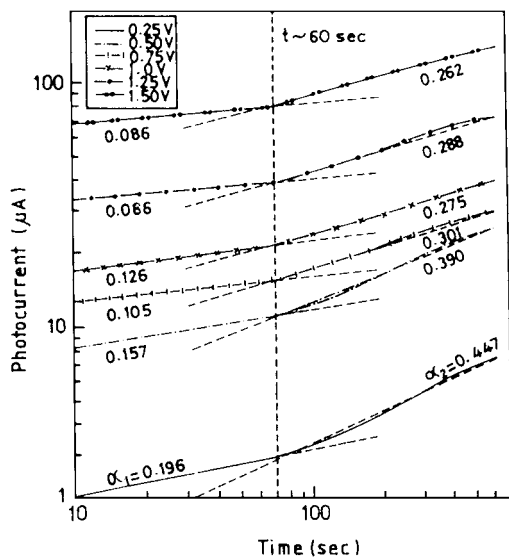


Figure 4 Logarithmic plot of the photocurrent growth with time for different bias voltages. Data has been taken from the rising portion i.e., M to N of Fig. 3. A linear variation of $\ln I_{ph} - \ln t$ indicates power law relation of photocurrent with time. It is observed that a change in slope occurs around a time of the order of 60 seconds.

is studied separately and discussed in subsequent sections. An initial attempt has been made to explain the experimental data with a theoretical model.

To investigate the photocurrent growth the rising portion (from M to N) of Fig. 3 is plotted separately. It is found that the growth of photocurrent with time has a rich structure and is distinctly different from a simple exponential one. The $\ln I_{ph} - \ln t$ plot in Fig. 4 shows a linear variation indicating a power law relation of photocurrent with time with two distinct portions. It is further observed from Fig. 4 that a sudden change in slope occurs around a time of the order of 60 seconds which does not alter with bias voltage. The photocur-

TABLE I Values of A's and α 's with bias voltage during photocurrent growth

Bias voltage (V)	Growth process			
	$t < 60 \text{ sec}$		$t > 60 \text{ sec}$	
	A_1	α_1	A_2	α_2
0.25	1.228	0.196	0.428	0.447
0.50	5.774	0.157	2.123	0.390
0.75	10.007	0.105	4.381	0.301
1.00	12.736	0.126	6.843	0.275
1.25	27.368	0.086	11.624	0.288
1.50	55.933	0.086	26.833	0.262

rent growth is fitted with a power law of the following form

$$I_{ph} \sim A_1 t_1^{\alpha_1} \quad \text{for } t < t_g$$

$$\sim A_2 t_2^{\alpha_2} \quad \text{for } t > t_g \quad (4)$$

where the characteristic time, $t_g \sim 60 \text{ sec}$.

The values of the constants A's and α 's are estimated from the plot (Fig. 4). The values of these constants for different bias voltages are given in Table I.

From Table I it is seen that the values of the constants A's and α 's depend on the bias voltage. As the bias voltage increases the value of the constants A_1 and A_2 increase whereas the constants α_1 and α_2 decrease.

The portion indicated from N to O of Fig. 3 shows that the photocurrent attains a saturation value and becomes independent of time.

After attaining the saturation value the light is switched off and the photocurrent begins to decrease and after some times reaches the initial dark value. In Fig. 5 the $\ln I_{ph} - \ln t$ plot for the portion O to P shows a linear relationship with two distinct regions which indicates that the photocurrent decay also, similar to that of growth, does not occur exponentially with time. Again

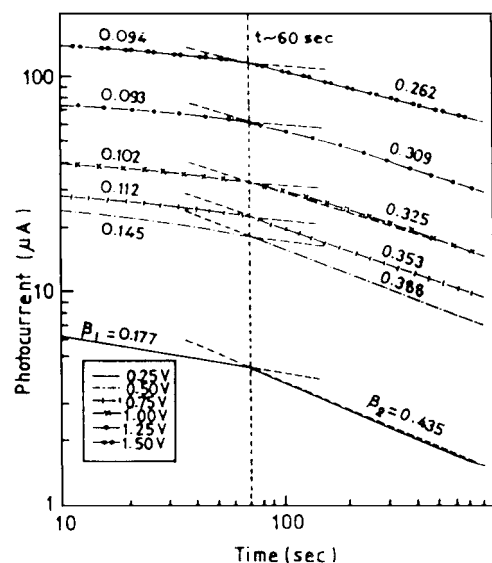


Figure 5 Logarithmic plot of decay of photocurrent with time for different bias voltage. Data taken from the portion O to P of Fig. 3. The $\ln I_{ph} - \ln t$ plot shows a linear relationship indicating a power law relation for the variation of photocurrent with time and it is observed that a change in slope occurs around a time of the order of 60 seconds for all bias voltage.

TABLE II Values of B's and β 's with bias voltage during photocurrent decay

Bias voltage (V)	Decay process			
	$t < 60$ sec		$t > 60$ sec	
	B ₁	β_1	B ₂	β_2
0.25	9.608	0.177	28.509	0.435
0.50	34.127	0.145	96.134	0.388
0.75	36.539	0.112	101.393	0.353
1.00	50.325	0.102	131.600	0.325
1.25	92.005	0.093	232.757	0.309
1.50	178.105	0.094	357.601	0.262

a change in slope is observed around a characteristic time, which again is of the order of 60 seconds and this is also found to be independent of the bias voltage. The decay of the photocurrent follows a power law of the form given by

$$I_{\text{ph}} \sim B_1 t_1^{-\beta} \quad \text{for } t < t_d$$

$$\sim B_2 t_2^{-\beta} \quad \text{for } t > t_d \quad (5)$$

where the characteristic time $t_d \sim 60$ sec.

The values of the constants B's and β 's estimated from Fig. 5 are given in Table II. From Table II it is observed that the constant B's and β 's are dependent on bias voltage and the constants B₁ and B₂ increase whereas the exponents β_1 and β_2 decrease with increasing bias voltage.

In order to understand qualitatively the behaviour of the photocurrent we may, to a first approximation, model the present system to be a disordered one with a distribution of scattering centers. In disorder amorphous organic materials charge carriers are highly localized and during transport the charge trapping occurs via hopping process. There will be a distribution of the energy levels of the localized hopping sites as well as a distribution in the intersite separation distances between them. As a consequence there is a distribution of hopping times. A dispersive model envisaging this idea originally suggested by Scher and Montrol [23] and has been further developed by other workers [19–22]. Both the factors mentioned above strongly affect the hopping time. Scher and Montrol [23] have specifically suggested a distribution function $\Psi(t)$ of the following form,

$$\Psi(t) \sim t^{-(1+\alpha)}, \quad 0 < \alpha < 1 \quad (6)$$

where t is time and α is the dispersion parameter which is a measure of the dispersivity. Unlike an asymptotic exponential tail with a single transition rate ($\Psi(t) \sim e^{-\lambda t}$, where λ is the finite rate) the above relation indicates hopping time dispersion. The long tail of $\Psi(t)$ causes a slow decay of the probability of long hopping times. Thus, at the beginning, fast processes will prevail, whereas slower charge dynamics will dominate the propagation on long time scales, leading to an increasing immobilization of charge carriers.

The essential point in the above dispersive transport model is that every charge carrier does not follow the same history before disappearance. Now in order to

describe the transient photocurrent behaviour in this model the mobility (μ_D) can be taken of the following form [41]

$$\mu_D(t) \propto \mu_0 t^{(\alpha-1)} \quad (7)$$

where μ_0 is the free carrier mobility. Then using the standard form [19] the photocurrent is written as a function of time as follows

$$I_{\text{ph}}(t) = N(t)qE\mu_D(t) \quad (8)$$

where $N(t)$ is the concentration of carriers in the sample, q is the electronic charge, E is the electric field and $\mu_D(t)$ is a time dependent mobility defined by Equation 7.

Kurtz and Huges [19] have utilized the above dispersive transport model to derive an expression for the growth of photocurrent when the sample is exposed to continuous radiation. The expression for the dc photocurrent is given by

$$I_{\text{ph}}(t) \propto t^\alpha [1 - 1/3(t/t_c)^\alpha] \quad \text{for } t < t_c \quad (9a)$$

$$I_{\text{ph}}(t) \propto t_c^\alpha [1 - 1/3(t_c/t)^\alpha] \quad \text{for } t > t_c \quad (9b)$$

when the radiation is turned on at time $t = 0$ and t_c is a characteristic time and is found to be of the order of 600 sec and which is, of course, different from either t_g in Equation 4 or t_d in Equation 5.

So, for continuous radiation we may write from Equation 9a for the growth of photocurrent with time approximately as

$$I_{\text{ph}}(t) \sim t^\alpha \quad \text{for } t \ll t_c \quad (10a)$$

which is of the same form as Equation 4 found from the present experiment.

For continuous radiation the saturation of photocurrent as found from Equation 9b can be approximately written as

$$I_{\text{ph}}(t) \sim t_c^\alpha = \text{constant} \quad \text{for } t \gg t_c \quad (10b)$$

This equation explains the constant portion of the $I_{\text{ph}}-t$ curve, namely N to O in Fig. 3.

The decay of the photocurrent and dark discharge have been studied by different workers [41, 42]. The sample sandwiched between two plane parallel electrodes behaves like a capacitor. At the moment when light is switched off the photocarriers within the sample is maximum which contributes a maximum photovoltage. These charge carriers begin to move due to the applied field. It may be expected that due to sudden change i.e., switching off the illumination the surface charge changes drastically. The transient current analysis accounts for the time dependent flow of mobile charge carriers under the applied bias in the presence of traps, space charges etc. These charge carriers become trapped during transport. The Poisson's equation is solved for both free and trap charges with suitable boundary conditions. The photovoltage change with

time may be approximated as [42]

$$V(t) = (L^2/2\mu_d)(1/t) \quad (11)$$

where $V(t)$, L and μ_D are the photovoltage, the thickness of the device and the time dependent mobility.

Taking $\mu_D(t) \propto \mu_0 t^{(\alpha-1)}$ for dispersive transport in disorder system one gets from Equation 11,

$$V(t) \sim t^{-\alpha} \quad (12)$$

The photocurrent is measured across the sensing resistance. So, the photocurrent is proportional to voltage across the resistance and can be expressed as

$$I_{ph}(t) \sim t^{-\alpha} \quad (13)$$

Thus, the non-exponential photocurrent decay may be qualitatively explained by using Equation 13 which is identical with the form obtained from experiment and given by Equation 5.

Equations 10a, 10b and 13 qualitatively describe the behavior of the photocurrent, during growth, saturation and decay. Growth and decay of photocurrent with time shows a broad agreement with the simple dispersive transport envisaged in the present model. From our experiment it is interesting to note that for both growth and decay there is a sudden change of slope in the $I_{ph}-t$ curve at around 60 sec which we call the characteristic time. This change is reflected in the alteration of values of exponents α 's and β 's. The complete explanation of this mechanism is not understood at present. The exponents α 's and β 's are a sort of measure of the disorder of the system which is sensitive to both electric field and temperature. Change of these parameters may be an indication of structural transformation of the host materials. It is also observed from Table I. and Table II. that for $t < 60$ sec both for growth and decay the values of the exponents i.e., α_1 and β_1 and for $t > 60$ sec the values of α_2 and β_2 are comparable for any particular bias voltage. The values of A's, B's, α 's, β 's depend on the applied voltage whereas the characteristic time is independent of bias voltage. The characteristic time seems to be determined by contributions from all the constituents, namely, Safranine-T, PVA, PEO, EC and PC. Experiments are being planned to study the dependence of the different constants (i.e., A's, B's, α 's and β 's) on the bias voltage as well as the components and to understand the significance of the sudden change of slope.

It is also significant to note that the decay and growth times of photocurrent are quite large being of the order of 600 and 800 sec respectively. A plausible mechanism for this slow response is as follows. In our system both ions and the electronic charge carrier are present. Both the ionic and electronic components contribute to the photocurrent. A steady state is reached due to the drift and diffusion of both ionic and electronic current. The motions of the ions are blocked by the electrodes but it can move inside the PEC within the electrodes causing the change of internal electric field within the devices which again affects the electronic current. So, it is expected that the photocurrent variation indicates

a variation of both ionic well as the electronic current. The slow response speed is related to both the slow motion of the salt ions and the trapping of charge carriers. During illumination an excess of carriers is generated and a new equilibrium occurs causing a movement and redistribution of ions from its steady initial distribution without illumination. Similarly during the decay the salt ion diffuses back into the electrolyte to its initial position. In both cases the ionic motion is expected which is obviously a slower process than its electronic counterpart. Apart from the slow ionic mobility, trapping of the charge carrier in different trap levels in host materials also lowers the response speed of the device. The transport of the charge carriers in organic materials are governed by hopping process of carriers from site to site which is spatially and energetically distributed and is significantly affected by charge trapping at deep states due to the presence impurities, structural defects and localized imperfections caused by structural and energetic disorders of hopping sites. The transport of charge carriers suffers multiple trapping in host materials. During trapping the charge carriers are being immobilized. The immobilization of the charge carriers lead to a low mobility and cause slow transient photocurrent decay [43] response. Thus slow response time of this device is the result of slow diffusion of ions as well as the immobilization of the charge carriers in deep traps.

4. Conclusions

In this work photoconductivity study in Safranine-T dye doped polymer photoelectrochemical cell is described. The photoresponse is observed on application of an external bias voltage on the device illuminated by a tungsten lamp. The incident radiation is absorbed by Safranine-T dye and photocarriers are generated. Once the photocarriers are generated charge trapping, recombination processes etc., determine the observed photoconductivity. The present photoconductivity measurement provides information on complex charge transport processes in these materials.

For a proper understanding of the device performance and to have a better insight of the charge transport property the dark $I-V$ characteristic, photocurrent growth and decay have been studied. Dark $I-V$ characteristic is fitted as $I \sim V^{(m+1)}$. The value of m is 0.11 below the bias voltage 1.1 V which shows that upto this low bias voltage the conduction is ohmic and in high operating voltage above 1.1. V the value m is 2.04 which indicates that the conduction process is governed by exponential distribution of traps.

The power law dependence of photocurrent growth and decay show a dispersive transport mechanism. Using a dispersive transport model, attempts have been made to explain the experimental data. But still important differences exist between theory and experiment. The interesting finding in our experiment is that for both growth and decay there is a sudden change of slope around a characteristic time 60 sec which is independent of bias voltage. Further work is in progress for understanding the charge transport process in these disordered materials, which will help to develop photosensors in dye doped photoconducting cell.

Acknowledgements

The authors thank Prof. S. C. Bera and Prof. S. C. Bhattacharya, Department of Chemistry, Jadavpur University, Calcutta-32, for providing valuable suggestions to prepare the sample. Two of the authors S. K. Dey and R. Islam acknowledge the financial assistance of State Govt. of West Bengal, India, for providing them financial assistance.

References

1. P. M. BORSENERGER and D. S. WEISS, "Organic Photoreceptors for Imaging Systems" (Marcel Dekker, New York, 1993).
2. K. S. NARAYAN and TH. B. SINGH, *Appl. Phys. Lett.* **74** (1999) 3456.
3. G. YU, C. ZHANG and A. J. HEEGER, *ibid.* **64** (1994) 1540.
4. S. L. ROMAN, *Adv. Mater.* **12** (2000) 189.
5. Y. GANG, W. JIAN, J. MCELIVAN and A. J. HEEGER, *ibid.* **10** (1998) 1443.
6. L. S. ROMAN, W. MAMMO, L. A. A. PATTERSON, M. ANDERSON and O. INGANAS, *ibid.* **10** (1998) 774.
7. B. MALLICK, R. N. BERA, A. BHATTACHARJEE and A. K. CHAKRABORTY, *Syn. Met.* **97** (1998) 63.
8. M. STOLKA, in "Special Polymers for Electronics and Optoelectronics," edited by J. A. Chilton and M. T. Goosey (Chapman and Hall, London, 1995), Ch. 8.
9. M. FUNAHASHI and JUN-ICHI HANNA, *Appl. Phys. Lett.* **74** (1999) 2584.
10. F. FELLER and A. P. MONKMAN, *ibid.* **76** (2000) 664.
11. K. NAKAYAMA, M. HIRAMOTO and M. YOKOYAMA, *ibid.* **76** (2000) 1914.
12. S. SALAFSKY, W. H. LUBBERHUIZEN and R. E. I. SCHROPP, *Chem. Phys. Lett.* **290** (1998) 297.
13. S. C. SHIM, M. C. SUH, S. C. SUH, X. L. HUANG and E. K. SUH, *Polymer* **41** (2000) 467.
14. S. C. BHATTACHARYA, P. RAY and S. P. MOULIK, *J. PhotoChem. and PhotoBio. A.* **88** (1995) 139.
15. H. ANTONIADIS, B. R. HSIEH, M. A. ABKOWITZZ, S. A. JENEKHE and M. STOLKA, *Synth. Met.* **62** (1994) 265.
16. L. R. A. K. BANDARA, M. A. K. L. DASANAYAKE, G. V. K. EKANAYAKE, O. A. ELEPERUMA and T. T. K. WEERAMAN, *Sol. State Ionics: Sc. and Tech.* (2000) 493.
17. C. J. BARBEC and N. SERDAR SARICIFTCI, in "Semiconducting Polymers," edited by G. Hadziioannou and P. F. V. Hutten, (WILEY-VCH, New York, 1999), Ch. 15.
18. B. M. MANDAL, *J. Indian Chem. Soc.* **75** (1998) 121.
19. S. R. KURTZ and R. C. HUGHES, *J. Appl. Phys.* **54** (1983) 229.
20. S. R. KURTZ and C. ARNOLD, *ibid.* **57** (1985) 2532.
21. P. E. BURROWS, Z. SHEN, V. BULOVIC, D. M. MCCARTY, S. R. FOREST, J. A. CRONIN and M. E. THOMPSON, *ibid.* **79** (1996) 799.
22. P. MARK and W. HELFRICH, *ibid.* **33** (1962) 205.
23. H. SCHER and E. W. MONTRON, *Phys. Rev. B* **12** (1975) 2455.
24. S. K. DEY and N. B. MANIK, *Applied Biochemistry and Biotechnology* **96** (2001) 55.
25. S. K. DEY, N. B. MANIK, S. BHATTACHARYA and A. N. BASU, *Synthetic Metals* **118** (2001) 19.
26. A. J. BHATTACHARYA, S. BANERJEE, T. R. MIDDYA and S. TARAFDAR, *Fractals* **6** (1998) 285.
27. YONG CAO, QIBING PEI, MATS R. ANDERSSON, GANG YU and ALAN J. HEEGER, *J. Electrochem. Soc.* **114** (1997) L317.
28. GANG YU, YONG CAO, CHI ZHANG, YONGFANG LI, JUN GAO and ALAN J. HEEGER, *Appl. Phys. Lett.* **73** (1998) 111.
29. YANG YANG and QIBING PEI, *ibid.* **68** (1996) 2708.
30. G. YU, Q. PEI and A. J. HEEGER, *ibid.* **70** (1997) 934.
31. J. GAO, G. YU and A. J. HEEGER, *ibid.* **71** (1997) 1293.
32. YONGFANG LI, JUN GAO, DELI WANG, GANG YU, YONG CAO and ALAN J. HEEGER, *Syn. Met.* **97** (1998) 191.
33. I. H. CAMPBELL, D. L. SMITH, C. J. NEEF and J. P. FERRARIS, *Appl. Phys. Lett.* **72** (1998) 2565.
34. D. L. SMITH, *J. Appl. Phys.* **81** (1997) 2869.
35. J. C. DEMELLO, N. TESSLER, S. C. GRAHAM and R. H. FRIEND, *Phys. Rev. B* **57** (1998) 12951.
36. J. YANG and J. SHEN, *J. Appl. Phys.* **85** (1999) 2699.
37. M. A. LAMPERT and P. MARK, "Current Injection in Solids" (Academic, New York, 1970).
38. J. YANG and J. SHEN, *J. Appl. Phys.* **83** (1998) 7706.
39. *Idem.*, *ibid.* **84** (1998) 2105.
40. V. BALOVIC, V. B. KHALFIN, G. GU, P. E. BURROWS and S. R. FOREST, *Phys. Rev. B* **58** (1998) 3730.
41. T. TIEDJE and A. ROSE, *Solid State Commun.* **37** (1980) 49.
42. I. P. BATRA, K. K. KANANZAWA and H. SEKI, *J. Appl. Phys.* **41** (1970) 3416.
43. H. BASSLER, *Phys. Status Solidi B* **175** (1993) 15.

Received 6 November 2001
and accepted 2 July 2002